Supplementary Information

Interface-Engineered Z-Scheme $CoIn_2S_4/MoSe_2$ Heterostructure for Enhanced Charge Separation toward Bifunctional Photocatalytic H_2 Production and O_2 Reduction

Ravina Saini, Saloni Latiyan, Lakshya Kumar, Sasanka Deka*

Department of Chemistry, University of Delhi, North Campus, Delhi-110007, India

*Email: sdeka@chemistry.du.ac.in

Materials and Methods

Chemicals and reagents. Cobalt (II) nitrate hexahydrate [$Co(NO_3)_2.6H_2O$, 99.5%], indium (III) chloride [$InCl_3$], sodium molybdate (IV) dihydrate [$Na_2MoO_4.2H_2O$, 99.0%), thioacetamide (C_2H_5NS, 99.0%), hydrazine hydrate ($N_2H_2.H_2O$, 99%), and selenium powder were purchased from Sigma Aldrich USA. Absolute ethanol (99%) and isopropanol (99%) were purchased from Fischer-India. Cerium (IV) sulfate anhydrous (97%), ferroin Solution, hydrogen peroxide (30%), sulphuric acid (98%), sodium sulphide (55-58%), sodium Sulphite anhydrous (96%) was purchased from Sigma-Aldrich. All chemicals are of analytical grade and used as received without any further purification.

Materials Characterization techniques:

1. **Powder X-ray diffraction (XRD):** Using powder X-ray diffraction (XRD) measurement, the crystal structure and phase purity of the as-synthesised $CoIn_2S_4$, $MoSe_2$, and $CoIn_2S_4/MoSe_2$ were examined on a Rigaku ULTIMA IV X-Ray diffractometer by using Cu Kα radiation (λ = 0.154056 nm) source. Dried powder was deposited onto the sample holder for the XRD measurements.
2. **Atomic Force Microscopy (AFM):** AFM images were acquired on a Bruker Dimension Icon-XR scanning probe microscope. Morphology scans were taken in tapping mode under ambient conditions using RTESP-300 probes (Bruker; nominal spring constant ≈ 42 $N \cdot m^{-1}$, resonance ≈300 kHz). The instrument supports Peak Force/Peak Force-QNM, Fast Scan tapping, KPFM, and conductive AFM (CAFM) for simultaneous topographic, mechanical, and nanoelectrical mapping, and was used for

height, potential (KPFM), and current (CAFM/TUNA) measurements where indicated. Optical studies were done using a UV–vis Spectrophotometer (make and model Agilent Cary 5000, having wavelength range 175nm – 3300nm with a Double out–of–plane Littrow Monochromator, a light source: Tungsten–halogen and deuterium, and a detector: R 928 Photomultiplier).

3. **Field Emission Scanning Electron Microscopy (FESEM)**: Morphological characterisation was carried out using field emission scanning electron microscopy (FESEM, Gemini SEM 500 analyser at 20 kV) using 10 mg solid powder sample.
4. **Transmission electron microscopy (TEM):** All TEM imaging, including the high-resolution transmission electron microscopy imaging (HR-TEM), was recorded using a JEOL JEM-F200 (200 kV) multi-purpose transmission electron microscope. The samples for TEM analysis were prepared by depositing two drops of a dilute solution of nanocrystals onto carbon-coated Cu grids. The Quad-Lens Condenser System was used for STEM-Elemental Mapping of the atomic weight percent of different elements.
5. **X-ray photoelectron spectroscopy (XPS):** Samples for chemical analysis by X-ray photoelectron spectroscopy (XPS) were deposited and dried onto a titanium substrate and then analyzed using an Axis Supra instrument with monochromatic Al Kα X-ray (1486.7 eV).
6. **Brunauer-Emmett-Teller (BET):** Nitrogen adsorption-desorption analyses for surface area, pore size, and pore volume determination were carried out using the model Quantachrome AUTOSORB iQ equipment. The Brunauer-Emmett-Teller (BET) method was used for surface area Horvath-Kawazoe method was used for micropore analysis.
7. **UV-Vis Spectrophotometer:** Ultraviolet-visible spectra (UV-vis) of solid materials were recorded on an Agilent Cary 5000 spectrophotometer using a Wavelength range of 200 nm – 800 nm. Monochromator: Double out-of-plane Littrow Monochromator, Light source: Tungsten-halogen and deuterium, Detector: For UV-VIS: R 928 Photomultiplier were used.
8. **Photoluminescence (PL):** Photoluminescence (PL) measurements for the individual samples were carried out using an Agilent Cary 5000 spectrophotometer. A very dilute solution was prepared by dispersing 1–2 mg of the sample in 4 mL of distilled water to ensure optimal measurement conditions.
9. **Time Resolved Photoluminescence (TRPL):** This was performed on Up/Down conversion PL using Horiba Canada, Model: FL 1039A/40A. Time Decay in the

microseconds range was measured using a Xenon lamp, Time Correlated Single Photon Counting (TCSPC) (Model: NL-C2 Pulsed Diode Controller, NANO LED, make: Horiba Scientific), which can be done using a Nano LED Laser having a wavelength of 375-315nm for a solid powder sample.

10. **Electron Spin/Paramagnetic Resonance (ESR/EPR) Spectrometer:** This characterization were done using JEOL model: JES-X320, Sensitivity: 5 x 109 spins/0.1 mT, using powder sample type, having Standard Frequency: X-band: 8.75 – 9.65 GHz, Q-band: 34 – 36 GHz, Microwave oscillation source: Gunn diode oscillator, Frequency resolution: 10 kHz, Electromagnet: Magnetic Field Range: 1300 mT (1.3 T), Resolution: 2.35 μT, Magnetic Field Stability: 0.5 – 1.0 μT, Cavity Resonator: Resonance Mode: TE011 cylindrical, Resonator resonant frequency: 9450 MHz, Spectrometer: Frequency: 100 kHz, 50 kHz, 25 kHz, Magnetic field sweep width: ± 500 mT, Temperature dependent, Low Temperature Range: Upto -160 ˚C (liquid nitrogen).
11. **Ultraviolet Photoelectron Spectroscopy (UPS):** For individual $CoIn_2S_4$ and $MoSe_2$ samples, UPS measurements were performed using a THERMO SCIENTIFIC ESCALAB QXi instrument. Helium gas was employed as the excitation source. For sample preparation, a 1 cm × 1 cm glass slide was used as the substrate. A catalyst slurry was prepared by dispersing 20 mg of the catalyst in 2 mL of isopropanol and stirring overnight to ensure uniform mixing. The resulting slurry was then coated onto the glass slide using a brush and allowed to dry before measurement.
12. **Mott-Schottky plot (M-S plot) and Electrochemical impedance spectroscopy (EIS) Measurements:** A Metrohm Autolab 204 potentiostat, managed by NOVA software (Metrohm, Netherlands), was used to perform both measurements at room temperature. The conventional three-electrode setup consisted of an Ag/AgCl reference electrode (saturated with KCl), a platinum wire counter electrode, and a glass slide coated with FTO as the working electrode. The working electrodes were prepared by coating them with the samples. For this, 100 mg of the catalyst sample was dissolved in 0.975 mL of acetone, and 25 μL of PVDF binder was added to create the working electrode films. After 30 minutes of sonication, this mixture was uniformly dispersed. On the surface of glass slides coated with FTO, around 100 μL of the resultant ink was applied (1 cm^2). Following deposition, the films were dried for one hour at 60°C and then annealed for two hours at 200°C to improve their adherence to the substrate. After that, the electrodes were submerged in an aqueous solution of 0.5 M Na_2SO_4, which was used as the inert

electrolyte for the EIS as well as M-S plot measurements. The Mott-Schottky (M-S) plot can be obtained by the following formula:

$$\frac{1}{C_S^2} = \frac{2}{\varepsilon_0 \varepsilon_r q N_A} \left(V_{applied} - V_{fb} - \frac{K_B T}{Q} \right) \quad (2)$$

in which C_S is specific capacitance of our material, $\mathcal{E}_0$ is the permittivity of vacuum, $\mathcal{E}_r$ is relative permittivity (value used 4.7 related to sulphur and 5.17 related to selenium), q is the electron charge, N_A is the charge carrier density, E_{fb} is the flat band potential, k_B is the Boltzmann constant, T is the temperature, $V_{applied}$ is the electrode potential, and V_{fb} represents the flat band potentials of the material

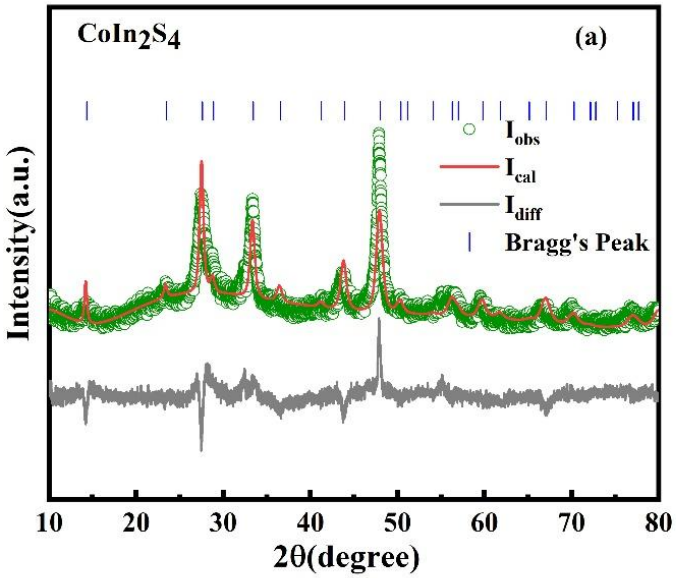

Fig. S1. Rietveld refinement for $CoIn_2S_4$.

Table S1. Refinement parameters from Fig. S1.

Catalysts	R_{wp} (%)	R_{exp} (%)	χ^2
$CoIn_2S_4$	7.38	5.36	1.56

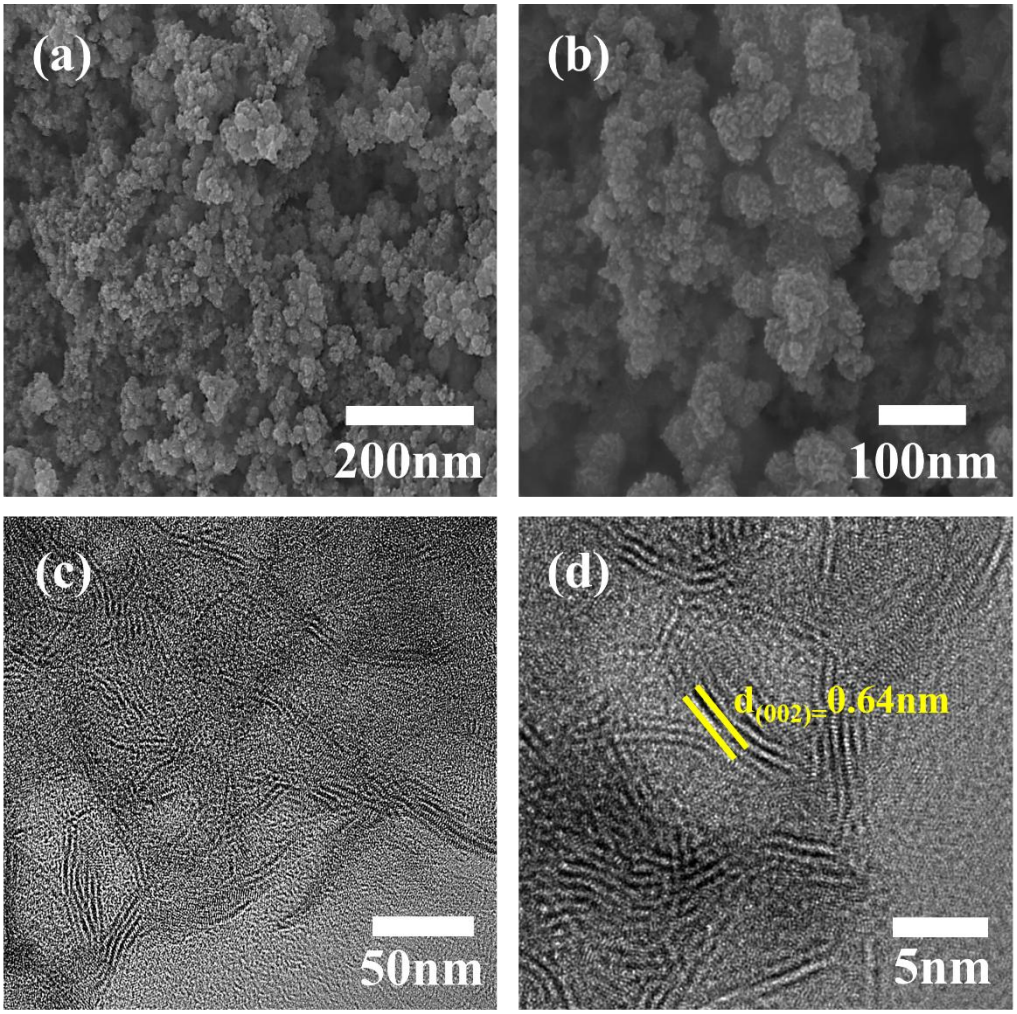

Fig. S2. (a, b) FESEM images of the $MoSe_2$ sample exhibiting an agglomerated nanourchin structure. (c, d) TEM and HR-TEM images of $MoSe_2$ showing a nanosheet.

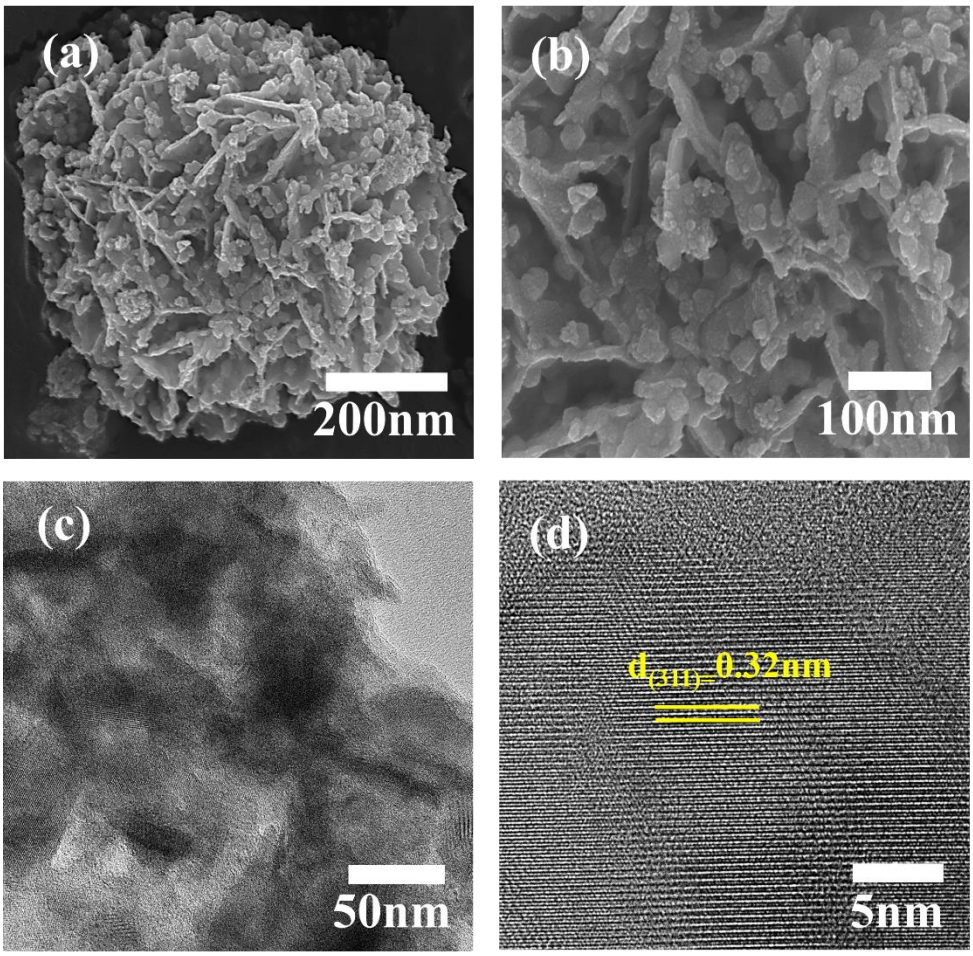

Fig. S3. (a, b) FESEM images of the $CoIn_2S_4$ sample exhibiting an agglomerated nanosheet structure. (c, d) TEM and HR-TEM images of $CoIn_2S_4$ showing nanosheet.

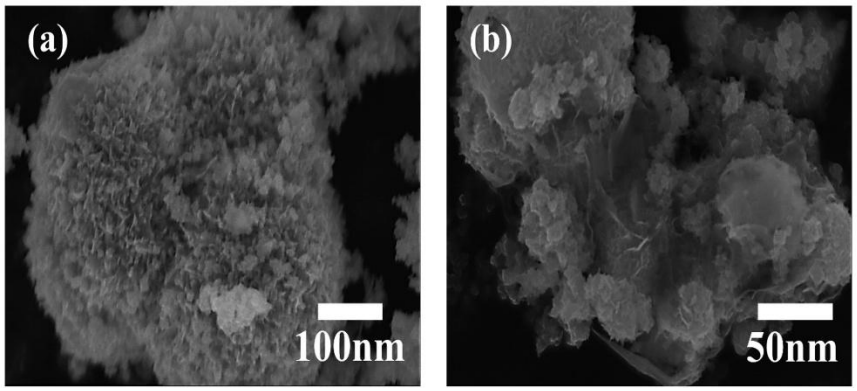

Fig. S4. (a, b) FESEM images of $CoIn_2S_4/MoSe_2$ sample exhibiting nanosheets that form a highly open three-dimensional hierarchical

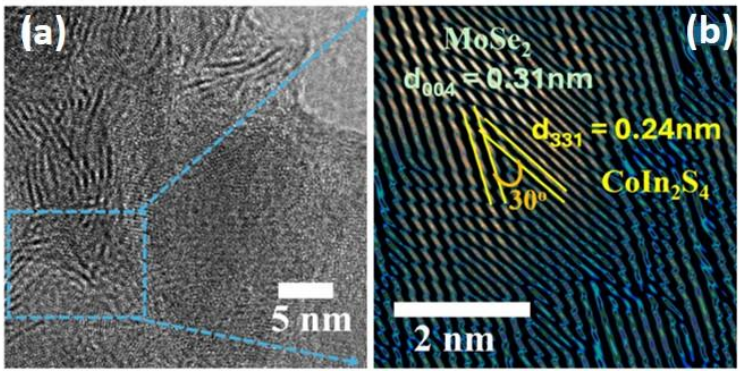

Fig. S5. (c) HRTEM image of $CoIn_2S_4/MoSe_2$ heterostructure and its (d) inverse FFT image showing growth of $CoIn_2S_4$ on $MoSe_2$.

Determination of the lattice mismatch:

The mismatch degree between the (400) plane of $CoIn_2S_4$ and the (002) plane of $MoSe_2$ was determined based on the following equation:

$$f = \frac{\alpha_s - \alpha_g}{\alpha_s} \times 100\% = \frac{d_s - d_g}{d_s} \times 100\%$$

The term, α_s and α_g represent the lattice constants, and d_s and d_g represent the lattice spacing of the two materials, respectively.

According to XRD and HRTEM results for **Fig. 1g**, the lattice spacing relationship between the (400) plane of $CoIn_2S_4$ and the (002) plane of $MoSe_2$ in CIS/MS is with an angle 72°. In theory, the d_s and d_g are 0.64 and 0.26 nm, respectively. Therefore, the d_g in there should be calculated to be 0.84 following the equation of $d_g = \frac{0.26}{cos72}$. Finally, the mismatch degree can be determined to be 31% based on the equation of $f = \frac{0.64-0.84}{0.64}$. The above calculation process can also be found in earlier literature.[1,2]

For **Fig. S5**, the (331) plane of $CoIn_2S_4$ and the (004) plane of $MoSe_2$ in CIS/MS are at an angle of 30°, with lattice spacing equal to 0.24 and 0.31nm, respectively.

Therefore, $d_g = \frac{0.24}{cos41} = 0.27$

Finally, $f = \frac{0.31-0.27}{0.31} \times 100\% = 12.9\%$

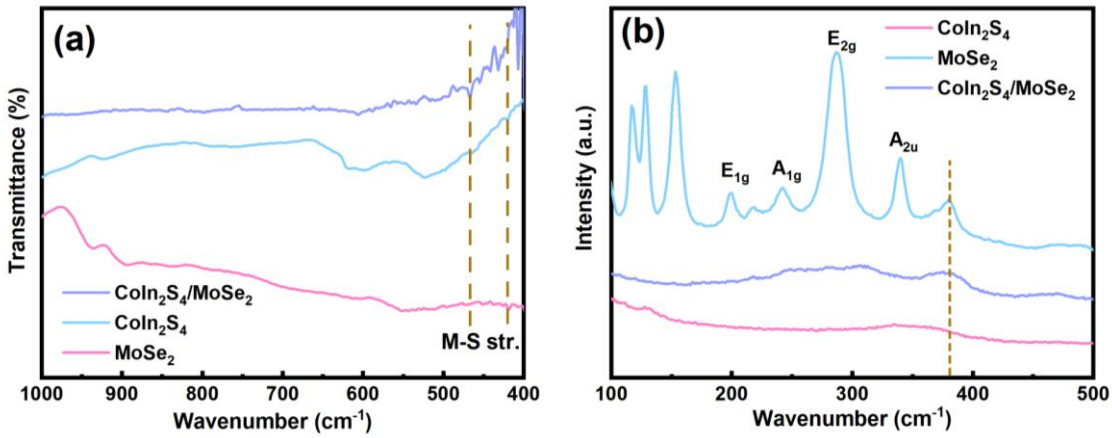

Fig. S6. (a) FT-IR, (b) RAMAN Spectra for samples as indicated.

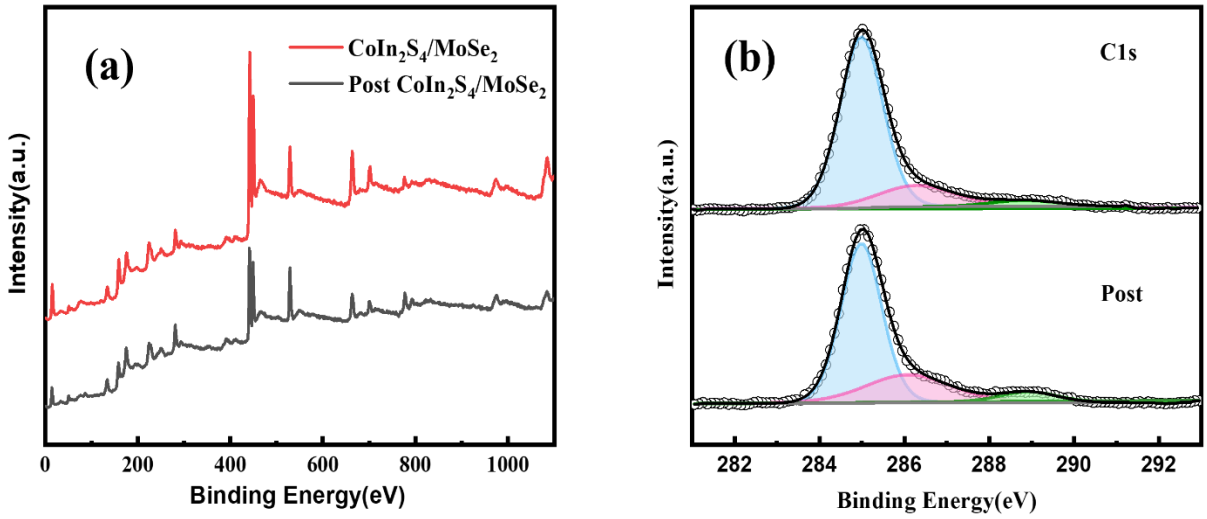

Fig. S7. (a) XPS Survey spectra of as-prepared $CoIn_2S_4/MoSe_2$ and $CoIn_2S_4/MoSe_2$ after 15h photocatalysis, High–resolution XPS: (b) C 1s.

Calculation of average lifetime:

The average lifetime (τ_a) can be determined using the following equation:

$$\tau_{a=} \frac{A_1\tau_1^2+A_2\tau_2^2+A_3\tau_3^2}{A_1\tau_1+A_2\tau_2+A_3\tau_3} \quad \text{(S1)}$$

Where A_1, A_2, A_3 and τ_1, τ_2, τ_3 are the amplitude and lifetime components, respectively.

Table S2. The decay lifetimes and the average lifetime of photoexcited charge carriers in $CoIn_2S_4$, $MoSe_2$ and $CoIn_2S_4/MoSe_2$ photocatalysts are listed below:

Sample	Amplitude components			Lifetime components (ns)			**Average life time (τ_a) ns**
	A_1	**A_2**	**A_3**	**τ_1**	**τ_2**	**τ_3**	
$CoIn_2S_4$	337.0	308.3	99.3	0.50	0.50	2.56	1.40
$MoSe_2$	48.1	343.9	-326.4	2.98	0.22	0.21	2.85
$CoIn_2S_4/MoSe_2$	336.8	273.5	182.3	0.44	0.43	10.41	9.18

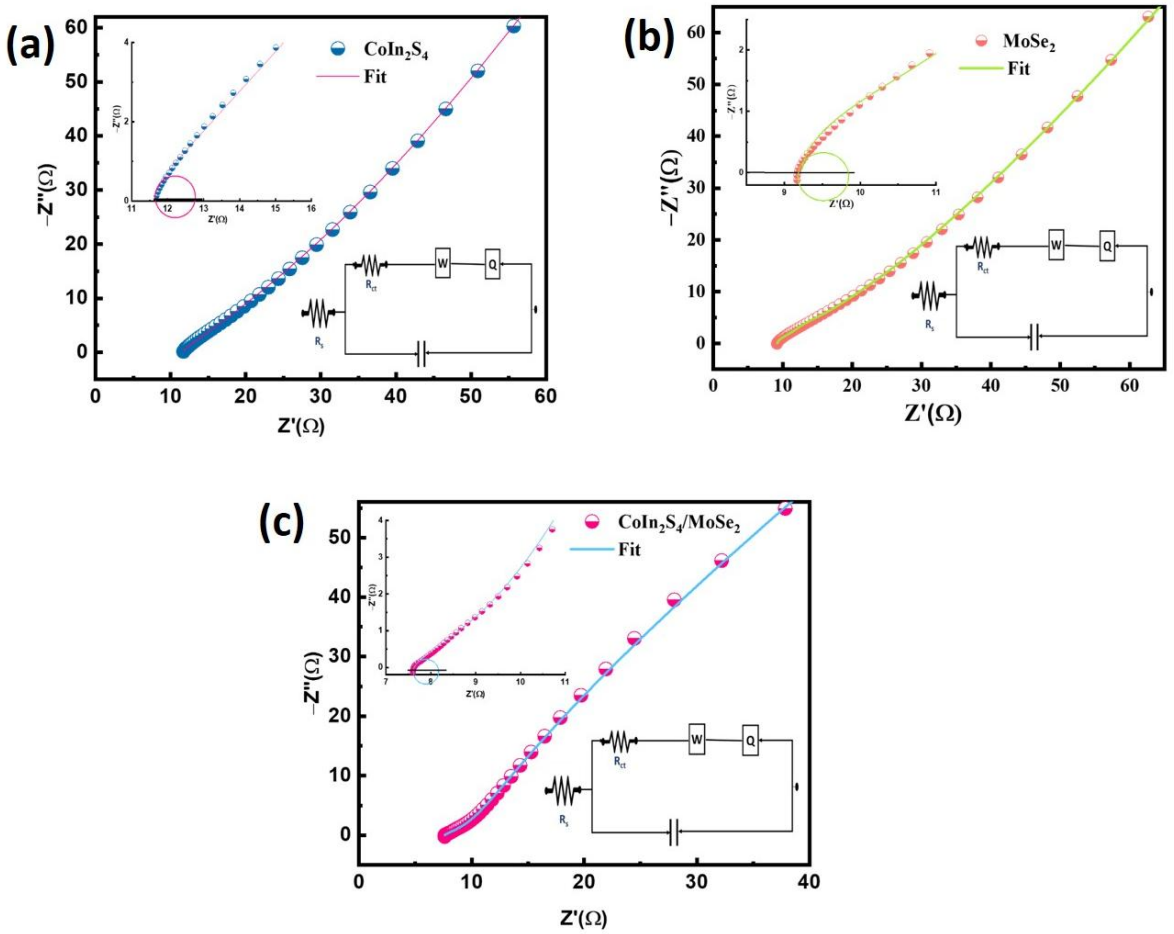

Fig. S8. Nyquist plots along with circuit diagram for (a) $CoIn_2S_4$, (b) $MoSe_2$, and (c) $CoIn_2S_4/MoSe_2$.

Table S3. Calculated EIS parameters from Fig. S7.

S. No.	Sample	R_s (Ω)	R_{ct} (Ω)	R_t (Ω)	C(μF)	W (m $\Omega^{-1}s^{1/2}$)	CPE Y_0 (F)
1.	$CoIn_2S_4$	11.6	12.8	24.4	28.4	1.87	1.1×10^{-4}
2.	$MoSe_2$	9.1	9.8	18.9	26.3	7.94	1.3×10^{-4}
3.	$CoIn_2S_4$/ $MoSe_2$	7.5	8.1	15.6	17.2	21.4	4.3×10^{-3}

Table S4. Surface area, pore volume, and pore size from BET measurements.

Sample	S_{BET} (m^2g^{-1})	Pore Volume (cm^3g^{-1})	Pore Size (nm)
$CoIn_2S_4/MoSe_2$	65.768	0.101	1.91
$CoIn_2S_4$	43.723	0.061	1.91
$MoSe_2$	41.742	0.075	1.90

Table S5. Types of different sacrificial reagents and the corresponding measured pH values.

S. No.	Sacrificial reagents	Measured pH
1	Ascorbic Acid	2.18
2	Na_2S/Na_2SO_3 (1:1)	12.93
3	TEOH (10%)	12.0
4	Methanol (10%)	7.50
5	Lactic acid (10%)	1.18

CALCULATIONS:

Determination of Donor Concentration (NA) of $CoIn_2S_4$ and $MoSe_2$ sample using slope from Mott-Schottky Plot.

$$\text{Slop} = \frac{2}{\varepsilon_0 \varepsilon_r q N_A}$$

Here,

ε_0 = permittivity of vacuum

ε_r = relative permittivity

q = electron charge

N_A = charge carrier density

k_B = Boltzmann constant and T = Temperature. This term k_BT is negligible (0.0244) in comparison to others.

For $CoIn_2S_4$:

$N_A = 2/8.85\times 10^{-10} \times 4.7 \times 1.602 \times 10^{-19}\times 2.50 \times 10^{8}$

$= \mathbf{1.2 \times 10^{19}\ cm^{-3}}$

For $MoSe_2$:

$N_A = 2/8.85\times 10^{-10} \times 5.17 \times 1.602 \times 10^{-19} \times 0.49 \times 10^{8}$

$= \mathbf{5.5 \times 10^{19}\ cm^{-3}}$

Photocatalytic Reaction

1. Rate of H_2 production

For $CoIn_2S_4/MoSe_2$:

0.0003024 mole h^{-1} = 0.3024 mmol h^{-1} = 302.4 μmol h^{-1} = 302.4/0.01 μmol $h^{-1}g^{-1}$ = 30,240 μmol $h^{-1}g^{-1}$

2. Number of H_2 molecules produced from $CoIn_2S_4$.:

The Volume of gas liberated in reaction in 1h = 3.0 ml = 0.003 L

Form std. gas equation PV= nRT

n = 0.003 L×1 atm / 0.082 L.atm mol^{-1} K^{-1} × 298 K

The corresponding amount of hydrogen in moles = 0.0001226 moles h^{-1}

1 mole gas = 6.023×10^{23} molecules

0.0001226 moles will have = $6.023 \times 10^{23} \times 0.0001226 = 7.39 \times 10^{19}$

H_2 molecule (per s) = $(6.023 \times 10^{23} \times 0.0001226) / (60 \text{ min} \times 60 \text{ s}) = 2.05 \times 10^{16}$

3. Number of H_2 molecule produced from $MoSe_2$:

The Volume of gas liberated in reaction in 1h = 4.9 ml = 0.0049 L

Form std. gas equation PV= nRT

n = 0.0049 L × 1 atm / 0.082 L.atm mol^{-1} K^{-1} × 298 K

The corresponding amount of hydrogen in moles = 0.0002005 moles h^{-1}

1 mole gas = 6.023×10^{23} molecules

0.0002005 moles will have = $6.023\times 10^{23} \times 0.0002005$

H_2 molecule (per s) = $(6.023 \times 10^{23} \times 0.0002005) / (60 \text{ min} \times 60 \text{ s}) = 3.35 \times 10^{16}$

4. Number of H_2 molecule produced from $CoIn_2S_4/MoSe_2$:

The Volume of gas liberated in reaction in 1h = 7.4 ml = 0.0074 L

Form std. gas equation PV= nRT

n = 0.0074 L × 1 atm / 0.082 L.atm mol^{-1} K^{-1} × 298 K

The corresponding amount of hydrogen in moles = 0.0003028 moles h^{-1}

1 mole gas = 6.023×10^{23} molecules

0.0003028 moles will have = $6.023\times 10^{23} \times 0.0003028$

H_2 molecule (per s) = $(6.023 \times 10^{23} \times 0.0003028) / (60 \text{ min} \times 60 \text{ s}) = 5.06 \times 10^{16}$

Table S6. Comparative assessment of robust photocatalysts and their H_2 Evolution characteristics.

Sr. No.	Catalysts	Light Source	Sacrificial reagents	H_2 Evolved ($\mu mol\ g^{-1}\ h^{-1}$)	Catalyst mass (in mg)	Ref.
1.	**$CoIn_2S_4/MoSe_2$**	**300W Xenon Lamp**	**0.35M/0.25M Na_2S/Na_2SO_3**	**30240**	**10**	**This Work**
2.	$Zn_{0.5}Cd_{0.5}S@ZnIn_2S_4/MoS_2$	300 W-Xe arc lamp	TEOA	8500	10	3
3.	covalent organic polymer COP-ZnIn2S4/Pt	300 W Xenon lamp	Na_2S/Na_2SO_3	5040	10	4
4.	$CdS/MoSe_2$	300 W Xe lamp	Na_2SO_4	25800	10	5
5.	$CdSe/NaNbO_3$	300 W Xe lamp	Na_2S/Na_2SO_3	2510	20	6
6.	$BiVO_4/ZnIn_2S_4$	300 W Xe lamp	TEOA	2243	50	7
7.	$NiTiO_3/TiO_2$	UV LED	Ethanol	11500	2.0	8
8.	$ZnIn_2S_4/MoSe_2$	300W Xenon Lamp	lactic acid	1748	5.0	9
9.	Co_3O_4 quantum dots /2D graphdiyne (g-C_nH_{2n-2})	5 W LED white-light	TEOA	1500.85	6.0	10
10.	LaCoO3/g-C3N4	300 W xenon lamp	methanol	1046.15	30	11
11.	ZnIn2S4@In(OH)3@CdS	300 W Xenon lamp	lactic acid	1384	30	12
12.	BP/BiVO4	300 W xenon lamp	No	160	5.0	13
13.	$CoIn_2S_4/g\text{-}C_3N_4$	300 W, $\lambda > 420$ nm	TEOA	62.701	50	14
14.	TiO_2/ZnTCuMT-X MOF	300 W xenon lamp	TEOA	3035.5	10	15
15.	$ZnIn_2S_4$-Au-TiO_2	300 W Xe lamp	No	186.3	50	16

5. Apparent quantum efficiency (AQE %) for H_2 production

$$AQE = \frac{2 \times nH_2}{Number\ of\ incident\ photons} = \frac{2.nH_2}{\frac{IA\lambda}{hc}} \times 100(\%)$$

Where, nH_2 is the number of H_2 molecules produced per second, I is the incident solar irradiance (W/cm^2) over the irradiated area A (cm^2), λ is the wavelength of the present study (nm), h Planck's constant and c is the speed of light.

$nH_2 = 5.06 \times 10^{16}$ per second

I = 2500 lux = 0.00275 W/cm^2

A = 50.2 cm^2

$$AQE = \frac{2 * 5.06 * 10^{16}}{(0.00275 * 50.2 * \boldsymbol{\lambda} * 10^{-9})/(6.626 * 10^{-34} * 3 * 10^{8})} \left(\frac{s^{-1}}{\frac{(\frac{W}{cm^2}.cm^2.m)}{j.s.m.s^{-1}}}\right) * 100\%$$

Table S7. Calculated AQE at the specified wavelength.

S. No.	Wavelength (nm) (λ value in the above equation)	AQE (%)
1	420	34.7
2	430	33.8
3	440	33.1
4	450	32.3
5	460	31.6
6	470	31.0
7	480	30.3
8	490	29.7
9	500	29.1
10	510	28.5
11	520	28.0
12	530	27.5

13	540	26.9
14	550	26.5
15	560	26.0
16	570	25.5
17	580	25.1
18	590	24.7
19	600	24.2

Average AQE = 27.7 %

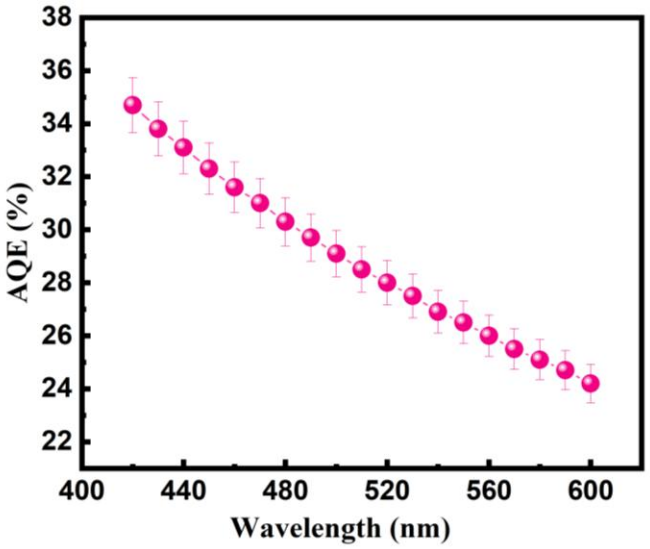

Fig. S9. Photocatalytic H_2 production: Apparent quantum efficiency of $CoIn_2S_4/MoSe_2$ (Photocatalyst: 10 mg; Photolyte: 30 mL of (1:1) Na_2S/Na_2SO_3 solution; light source: 300 W Xenon light).

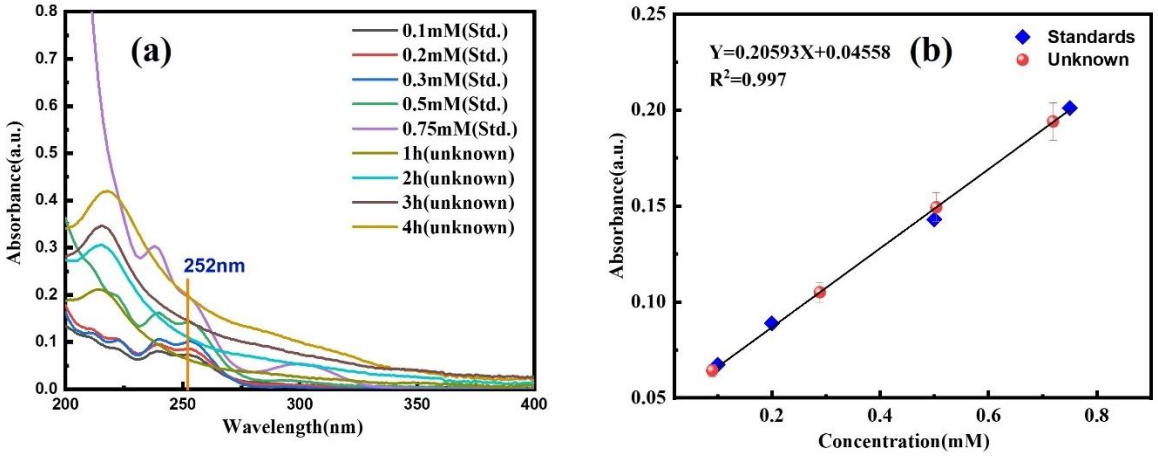

Fig. S10. (a) UV–Vis absorption intensity for various standard concentrations of H_2O_2 and unknown concentrations of H_2O_2 taken from the reactor after 1h interval using the titration method. (b) The linear calibration equation for the standard H_2O_2 concentrations.

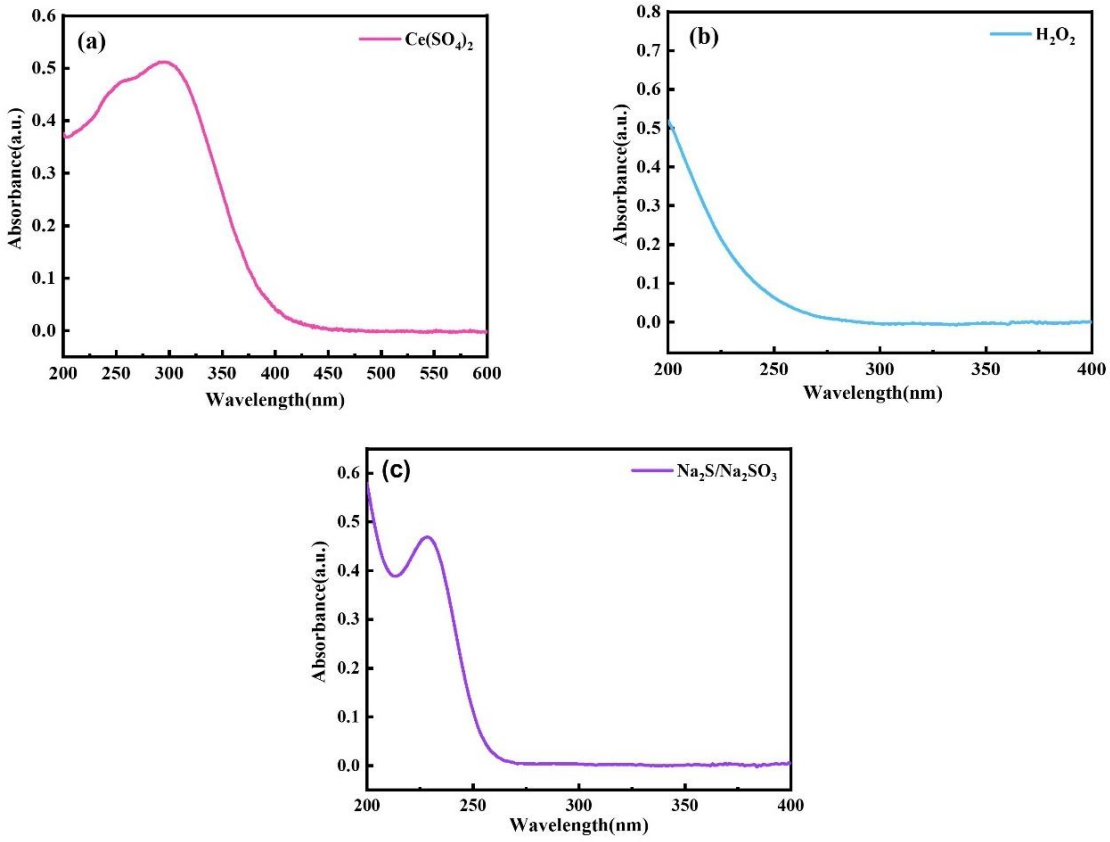

Fig. S11. UV–Vis absorption spectrum of (a) Cerium sulphate, (b) H_2O_2 and (c) Na_2S/Na_2SO_3.

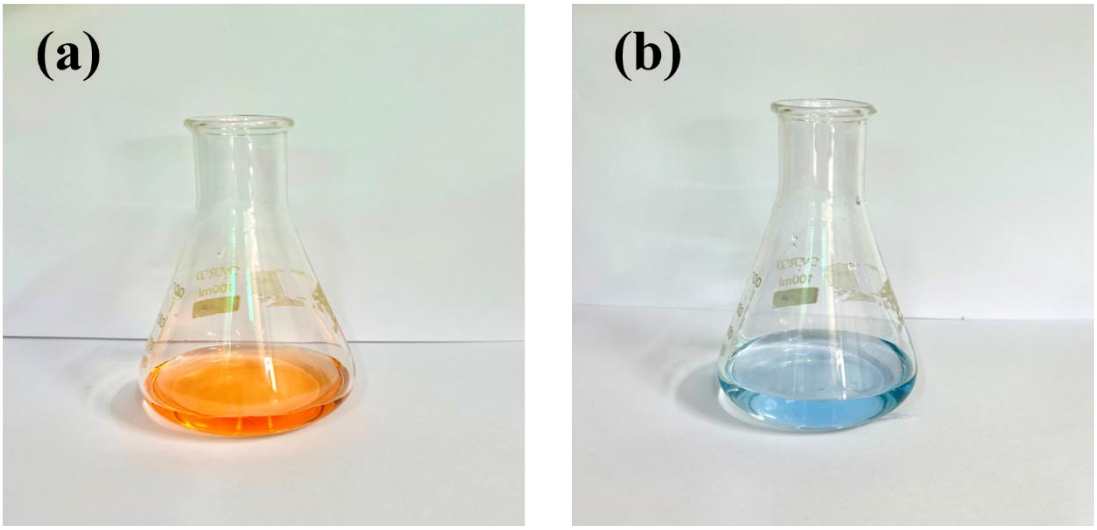

Fig. S12. Photographs of titration results in a color change from orange-red to blue–green. (a) before titration and (b) after titration.

Table S8. Comparison of reference photocatalysts and their efficiency in hydrogen peroxide (H_2O_2) production.

Sr. No.	Catalysts	Reaction condition	Light Source	H_2O_2 Production rate (mmol $g^{-1}h^{-1}$)	AQE(%)	Ref.
1.	**$CoIn_2S_4$/ $MoSe_2$**	**300W Xe Lamp**	**Water + 0.35M/0.25M Na_2S/Na_2SO_3**	**19.600**	**11.2**	**This work**
2.	ZnO/WO_3	300W Xe lamp	Water	6.788	12.5	17
3.	ZnO/g-C_3N_4	300W Xe lamp	Water	1.544	…	18
4.	KCN/ZnO	300W Xe lamp	Water + Ethanol	4.72	…	19
5.	$CoIn_2S_4$/ Ag_3PO_4	300W Xe lamp	Water	1.534	2.67	20
6.	$Bi_2O_3/ZnIn_2S_4$	300W Xe lamp	Water	0.600	…	21

Apparent quantum efficiency (AQE %) for H_2O_2 production:

$$AQE = \frac{2 \times nH_2O_2}{Number\ of\ incident\ photons} = \frac{2.nH_2O_2}{\frac{IA\lambda}{hc}} \times 100(\%)$$

$$AQE = \frac{2 * 1.63 * 10^{16}}{(0.00275 * 50.2 * \boldsymbol{\lambda} * 10^{-9})/(6.626 * 10^{-34} * 3 * 10^{8})} \left(\frac{s^{-1}}{\frac{(\frac{W}{cm^2}.cm^2.m)}{j.s.m.s^{-1}}}\right) * 100\%$$

Table S9. Calculated AQE at the specified wavelength.

S. No.	Wavelength (nm) (λ value in the above equation)	AQE (%)
1	420	11.2
2	430	10.9
3	440	10.7
4	450	10.4
5	460	10.2
6	470	10
7	480	9.8
8	490	9.6
9	500	9.4
10	510	9.2
11	520	9.0
12	530	8.9
13	540	8.7
14	550	8.5
15	560	8.4
16	570	8.2
17	580	8.1
18	590	7.9
19	600	7.8

Average AQE = 9.31 %

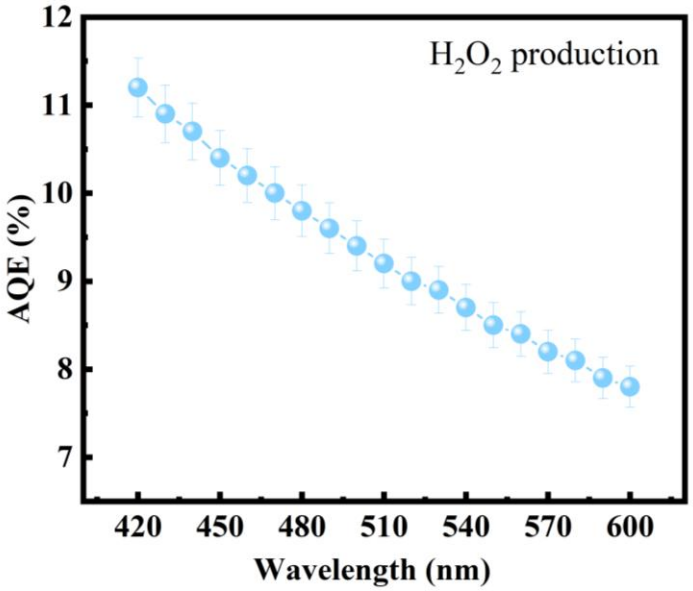

Fig. S13. H_2O_2 production: Apparent quantum efficiency of $CoIn_2S_4/MoSe_2$ (Photocatalyst: 5 mg; Photolyte: 5 mL of (1:1) Na_2S/Na_2SO_3 solution; light source: 300 W Xenon light).

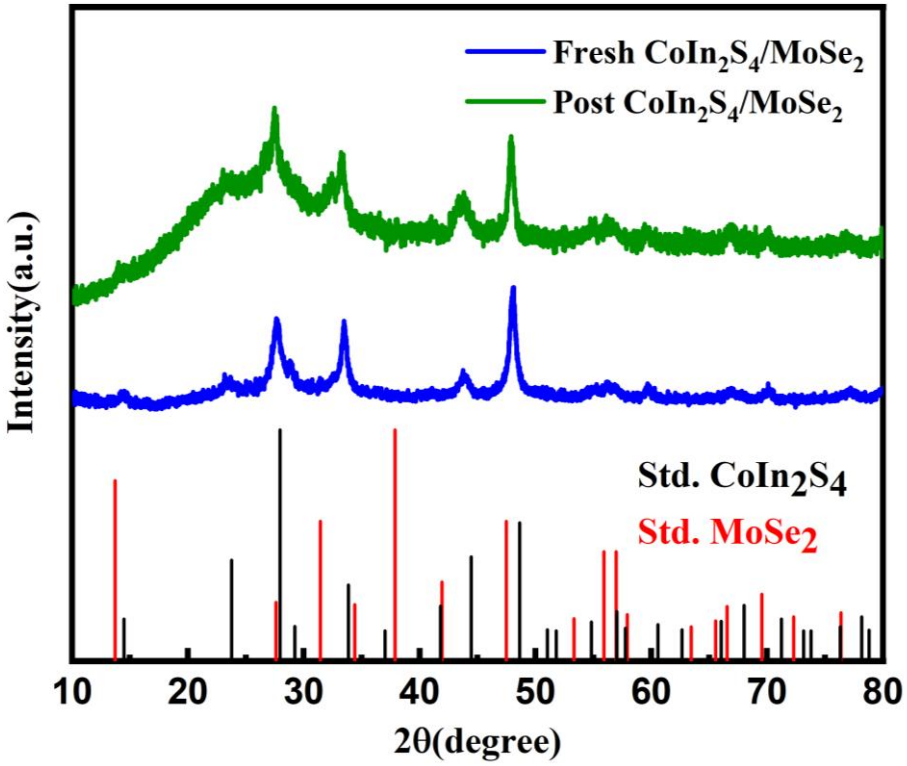

Fig. S14 Comparison of XRD patterns before and after photocatalytic H_2 production cycles.

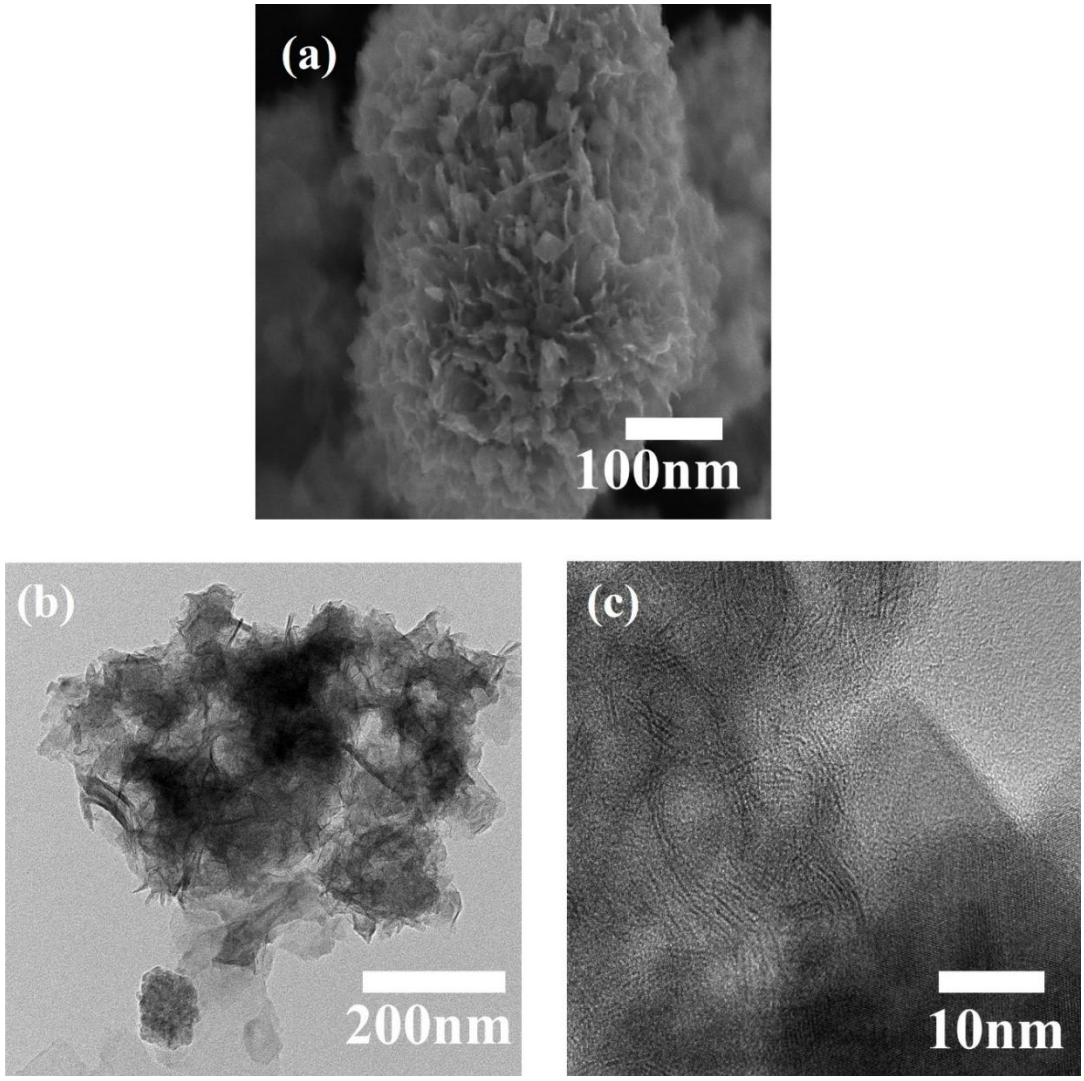

Fig. S15. (a) FESEM image and (b,c) TEM images of $CoIn_2S_4/MoSe_2$ after performing 15 h photocatalytic H_2 production reaction. (d) Comparison of XRD patterns before and after photocatalytic H_2 production cycles.

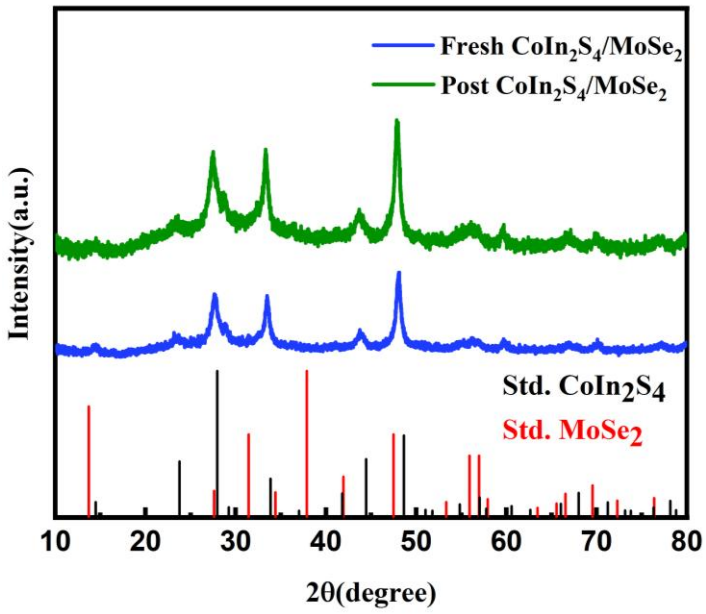

Fig. S16. Comparison of XRD patterns before and after photocatalytic H_2O_2 production cycles.

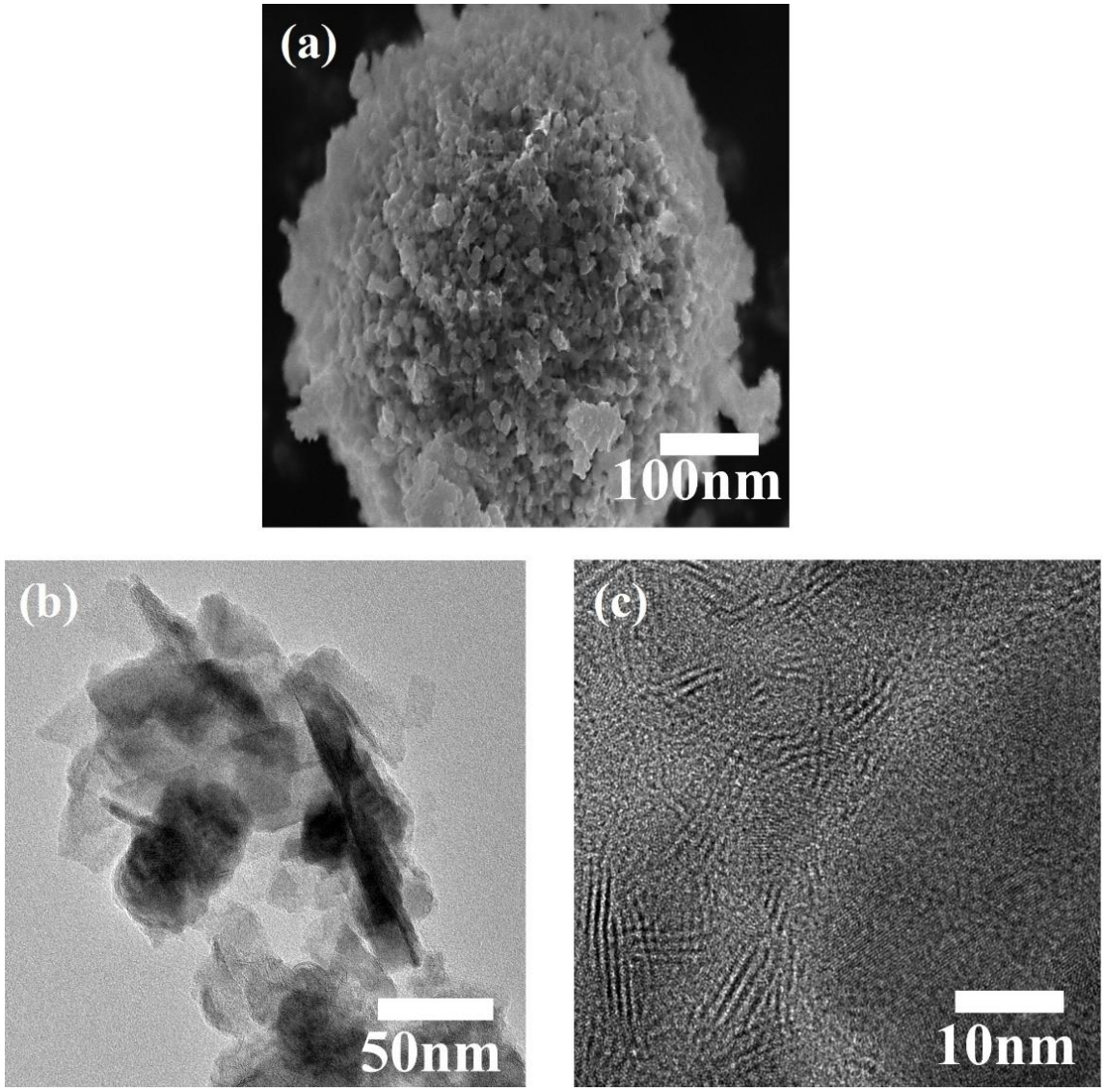

Fig. S17. (a) FESEM image, and (b,c) TEM images of $CoIn_2S_4/MoSe_2$ after performing a 4 h photocatalytic H_2O_2 production reaction.

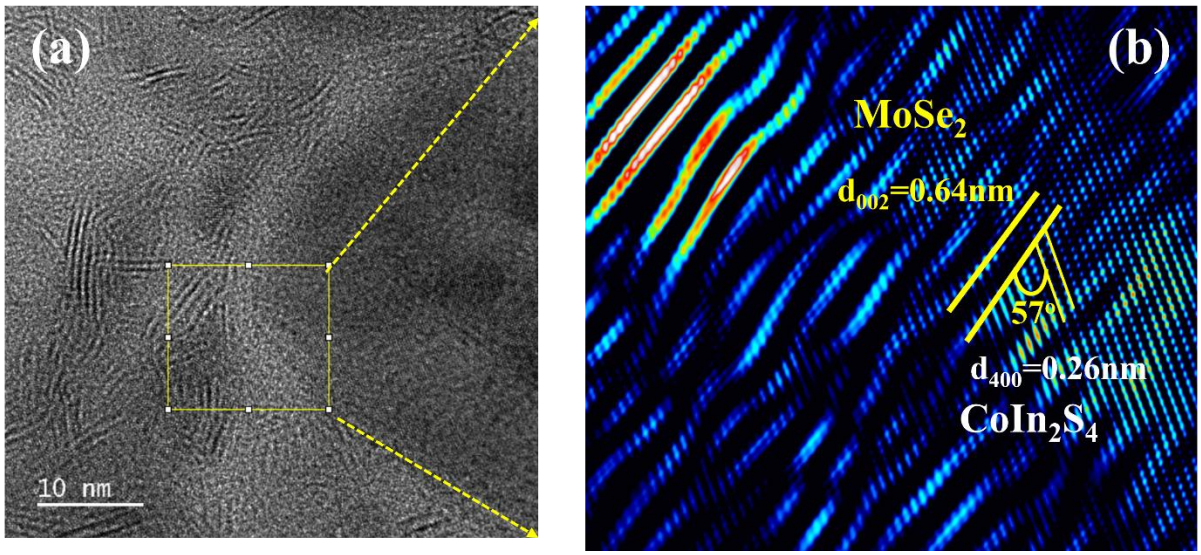

Fig. S18. (a) HRTEM image, and (b) Inverse FFT of HRTEM image of $CoIn_2S_4/MoSe_2$ after performing a photocatalytic reaction.

Here, the (400) plane of $CoIn_2S_4$ and the (002) plane of $MoSe_2$ in CIS/MS are at an angle of 57°, with lattice spacing equal to 0.64 and 0.26nm, respectively.

Therefore, $d_g = \frac{0.26}{cos57} = 0.47$

Finally, $f = \frac{0.64-0.47}{0.64} \times 100\% = 36.2\%$

References:

1. J. Zhang, X. Liang, C. Zhang, L. Lin, W. Xing, Z. Yu, G. Zhang and X. Wang, *Angew. Chem. Int. Ed.*, **2022**, 61, e202210849–e202210849.
2. X. Wang, T. Shi, X. Wang, A. Song, G. Li, L. Wang, J. Huang, A. Meng and Z. Li, *J. Energy Chem.*, **2024**, 92, 151–161.
3. Y. Ning, S. Wang, H. Wang, W. Quan, Daqi Lv, S. Yu, X. Hu and H. Tian, *J. Colloid Interface Sci.*, **2024**, 662, 928–940.
4. C. Cui, X. Zhao, X. Su, N. Xi, X. Wang, X. Yu, X. L. Zhang, H. Liu and Y. Sang, *Adv. Funct. Mater.*, **2022,** 32**,** 2208962.
5. C. Ding, C. Zhao, S. Cheng and X. Yang, *Surf. interfaces*, **202331**, 25, 101192–101192.

6. L. Gao, S. Chang, H. Gu, H. Zhang, Y. Huang, X. Wang, Q. Li and W. Dai, *ChemCatChem*, **2024,** e202400502.
7. L. Li, Z. Zhang, D. Fang and D. Yang, *Inorg. Chem. Commun.*, **2024**, 169, 112971.
8. C. Xing, Y. Liu, Y. Zhang, J. Liu, T. Zhang, P. Tang, J. Arbiol, L. Soler, K. Sivula, N. Guijarro, X. Wang, J. Li, R. Du, Y. Zuo, A. Cabot and J. Llorca, *J. Mater. Chem. A*, **2019**, **7**, 17053–17059.
9. M.-Q. Yang, Y.-J. Xu, W. Lu, K. Zeng, H. Zhu, Q. Xu and Ghim Wei Ho, *Nat. Commun.*, **2017**, 8, 14224.
10. D. Xiang, X. Hao, X. Guo, G. Wang, K. Yang and Z. Jin, *Adv. Mater. Interfaces*, **2022**, 9, 2201400.
11. R. Wang, C. Ye, H. Wang and F. Jiang, *ACS omega*, **2020**, 5, 30373–30382.
12. L. Ma, C. Lin, W. Jiang, L. Xu, Y. Shao, T. Zhu, T. Zhao, X. Ai and X. Wu, *Int. J. Hydrog. Energy*, **2024**, 57, 290–300.
13. M. Zhu, Z. Sun, M. Fujitsuka and T. Majima, *Angew. Chem. Int. Ed.*, **2018**, 57, 2160–2164.
14. C. Zeng and Y. Hu, *Nanotechnol.*, **2020**, 31, 505711–505711.
15. W. Zhu, H. Zhu, T. Zhang, L. Qin, S. Kang and X. Li, *Small*, **2024**, 21, e2408806–e2408806.
16. G. Yang, H. Ding, D. Chen, J. Feng, Q. Hao and Y. Zhu, *Appl. Catal. B: Environ.*, **2018**, 234, 260–267.
17. Z. Jiang, B. Cheng, Y. Zhang, S. Wageh, A. A. Al-Ghamdi, J. Yu and L. Wang, *J. Mater. Scie. Technol.*, **2022**, 124, 193–201.
18. B. Liu, C. Bie, Y. Zhang, L. Wang, Y. Li and J. Yu, *Langmuir*, **2021**, 37, 14114–14124.
19. H. Liang, J. Zhao, Angeliki Brouzgou, A. Wang, S. Jing, P. Kannan, F. Chen and Panagiotis Tsiakaras, *J. Colloid Interface Sci.*, **2024**, 677, 1120–1133.
20. Z. Ren, Q. Ren, Y. Li, H. Li, X. Zhang, M. Wang and X. Liu, *J. Alloys Compd.*, **2025**, 1036, 182123.
21. M. Xu, J. Ye, Z. Fan, J. Li, Y. Dai, Y. Xie, Y. Chen, S. Li and J. Zhang, *Sep. Purif. Technol.*, **2025**, 376, 134163–134163.

****